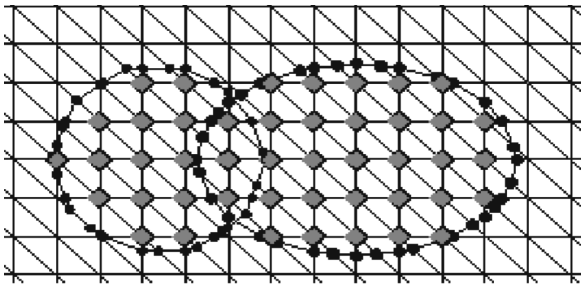

Figure 1. Two snakes colliding with the inside grid nodes and snake point (*snaxels*) marked. Reprinted with permission from Giraldi GA, Strauss E, Oliveira AF. 2003. Dual-T-snakes model for medical imaging segmentation. *Pattern Recognit Lett* **24**(7):993–1003. Copyright ©2003, Elsevier.

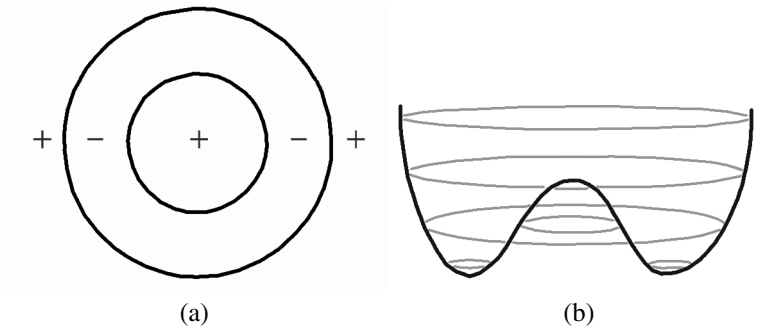

Figure 2. (a) Dual snakes bounding the search space. (b) Initial function where the zero level set is the two contours presented.

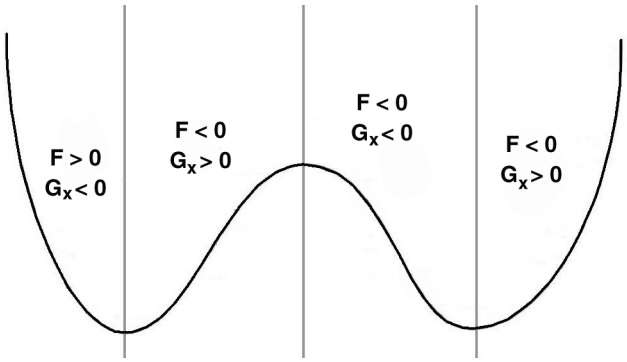

Figure 3. Sign of the speed function.

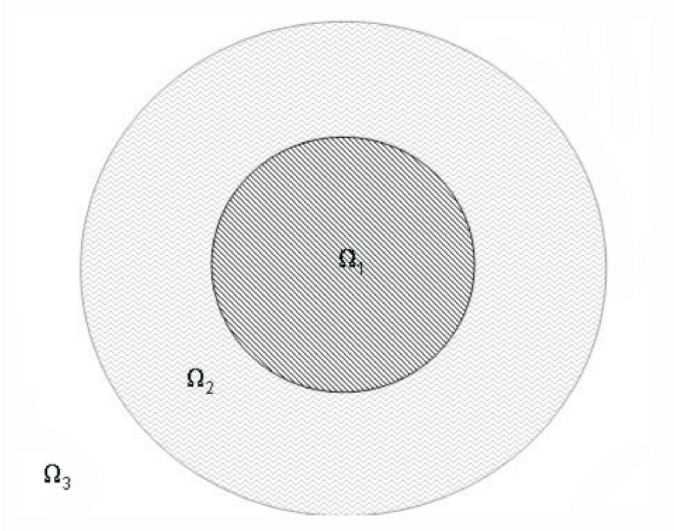

Figure 4. Support of a step function given by Eq. (41) with $a_1 = 1$, $a_2 = -1$, and $a_3 = 1$.

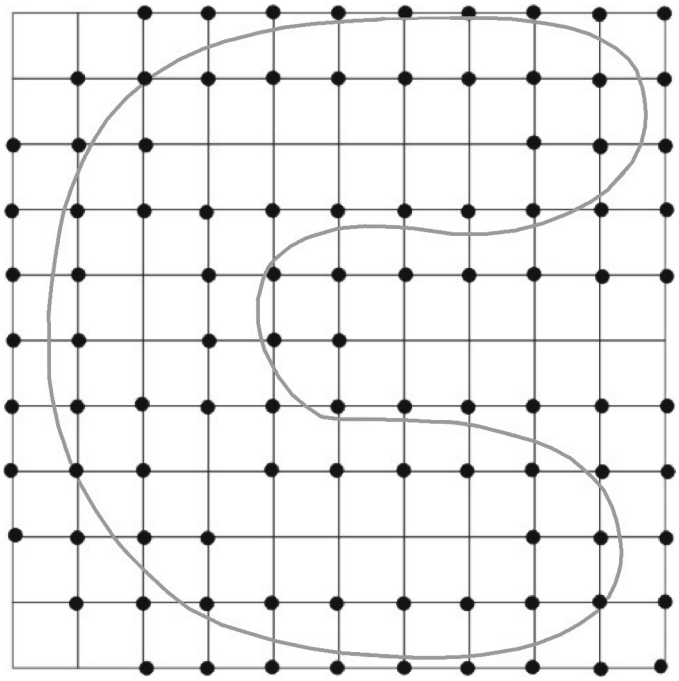

Figure 5. Narrow band around a propagating front.

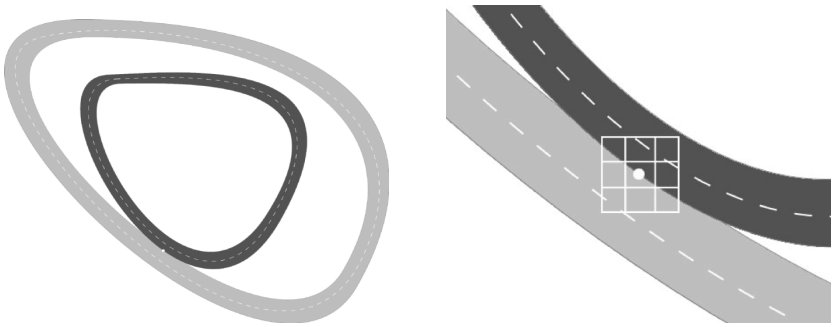

(a) (b)

Figure 6. (a) Narrow bands touching each other. (b) Neighborhood to define similarity between fronts.

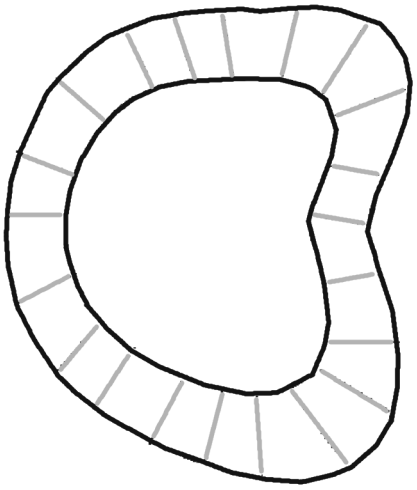

Figure 7. Search space obtained through a matching between inner and outer snakes.

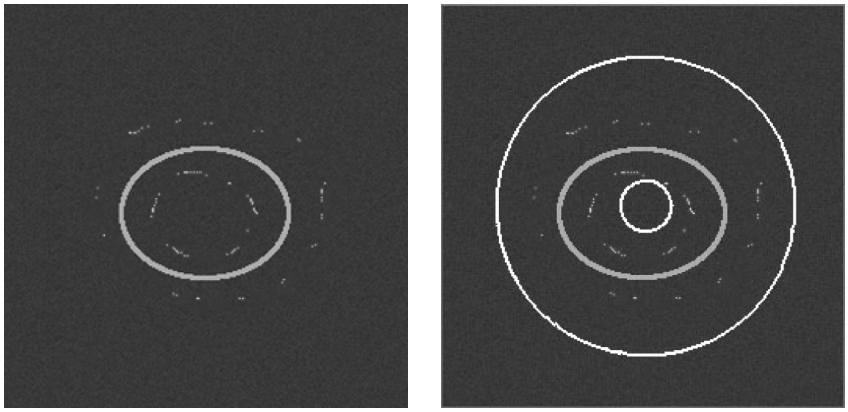

(a) (b)

Figure 8. (a) Original image. (b) Initial fronts.

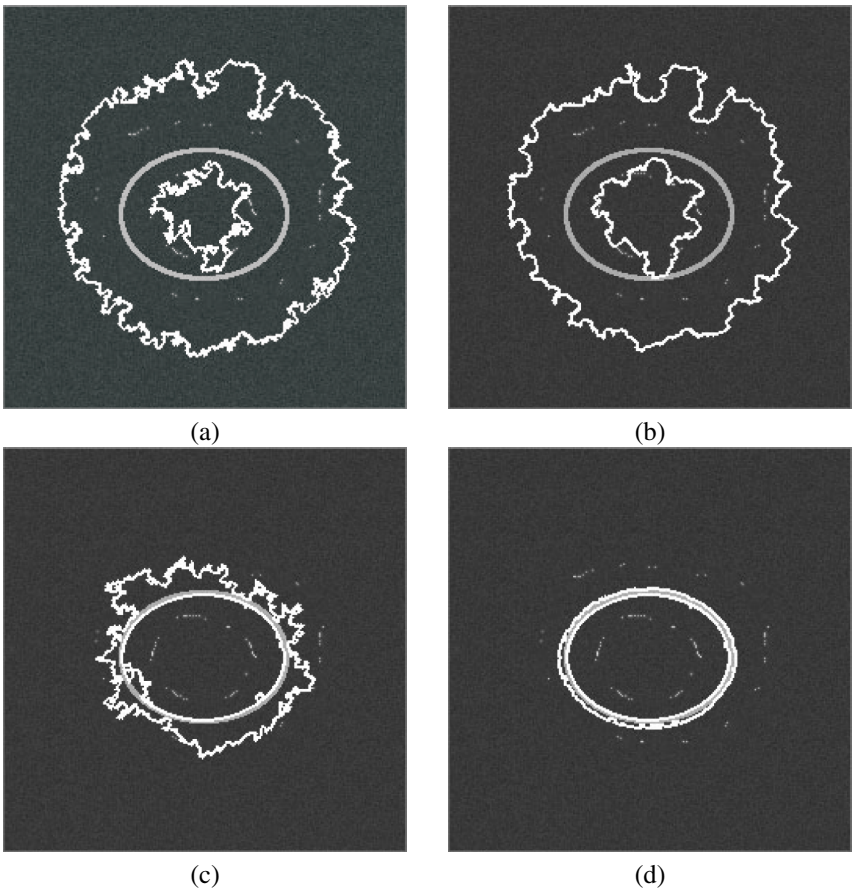

Figure 9. (a) Fronts stop moving at interaction 453 due to the low-velocity criterion. (b) Front position in interaction 463 when the stopping term is turned on. (c) Configuration at interaction 1347. (d) Final front positions.

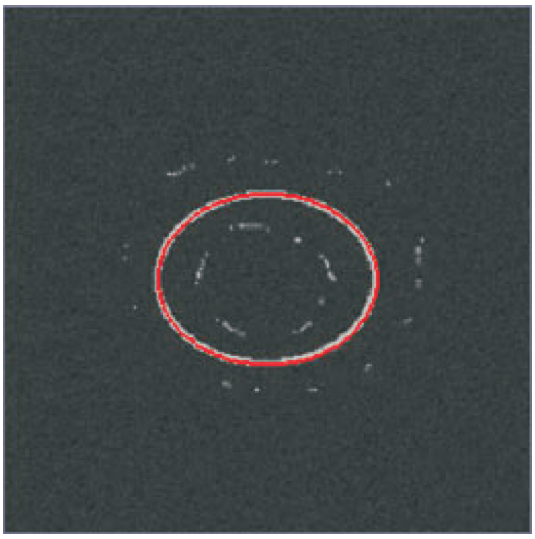

Figure 10. Final result obtained with the greedy snake model.

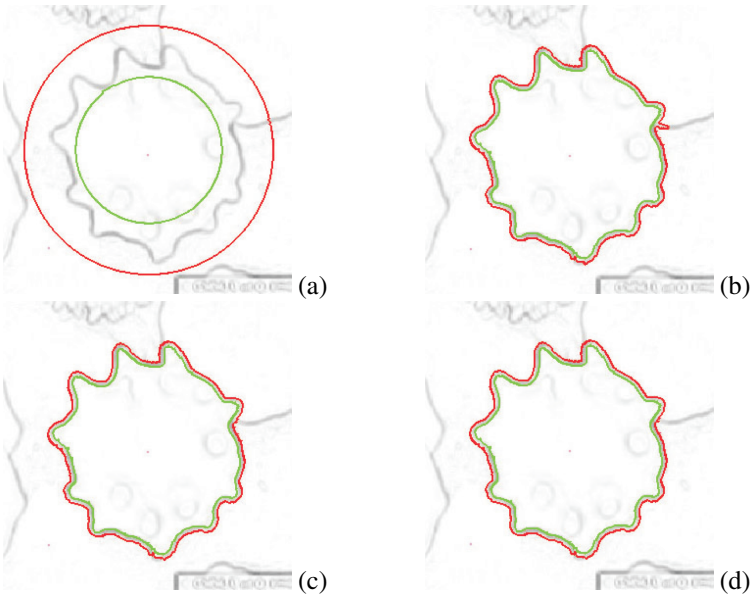

Figure 11. (a) Image and initial fronts. (b) Bandpass-filtered image and initial fronts. (c) Fronts stop moving at interaction 534 due to the low-velocity criterion. (d) Dual-Level-Set result obtained after 641 interaction steps.

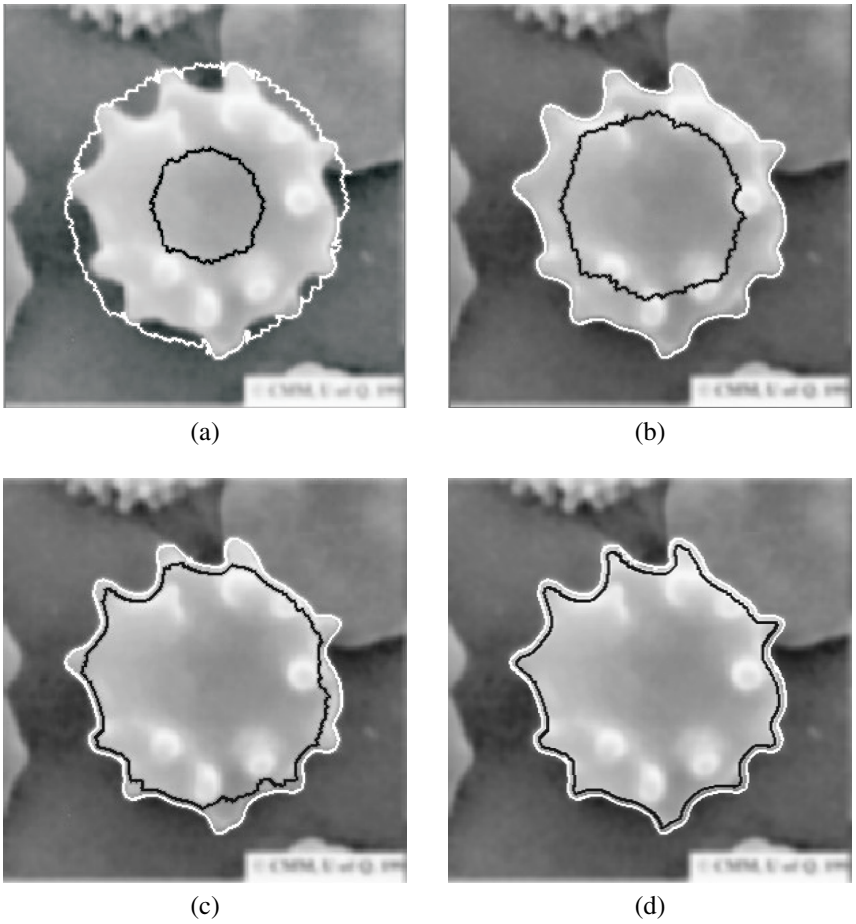

Figure 12. (a) Position of the fronts at interaction 200. (b) Interaction 400. (c) Fronts in interaction 600. (d) Dual-Level-Set result obtained after 926 interaction steps. Reprinted with permission from Giraldi GA, Strauss E, Oliveira AF. 2003. Dual-T-snakes model for medical imaging segmentation. *Pattern Recognit Lett* **24**(7):993–1003. Copyright ©2003, Elsevier.

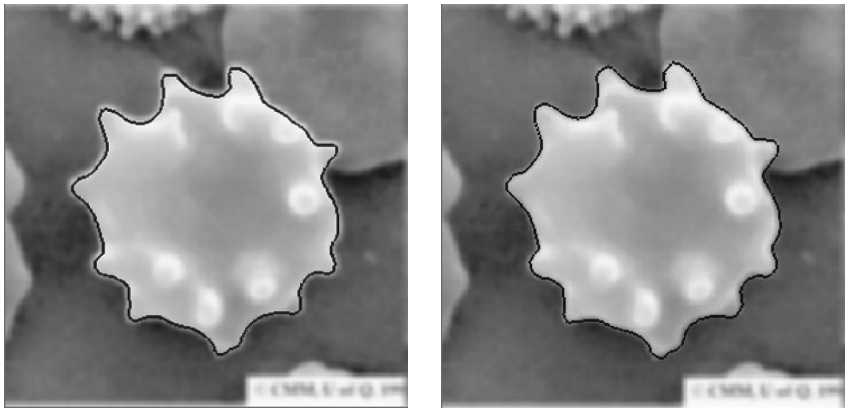

(a) (b)

Figure 13. (a) Initialization of the greedy snake model. (b) Final result. Adapted with permission from Giraldi GA, Strauss E, Oliveira AF. 2003. Dual-T-snakes model for medical imaging segmentation. *Pattern Recognit Lett* **24**(7):993–1003. Copyright ©2003, Elsevier.

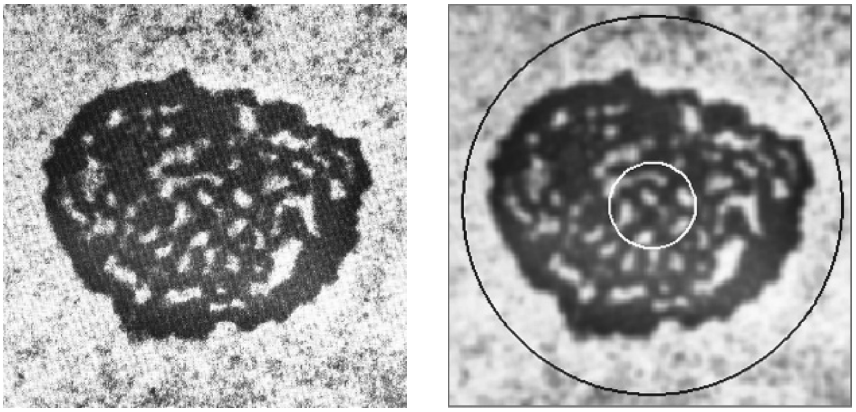

(a) (b)

Figure 14. (a) Original image with a cell nucleolus. (b) Initial fronts. Adapted with permission from Giraldi GA, Strauss E, Oliveira AF. 2003. Dual-T-snakes model for medical imaging segmentation. *Pattern Recognit Lett* **24**(7):993–1003. Copyright ©2003, Elsevier.

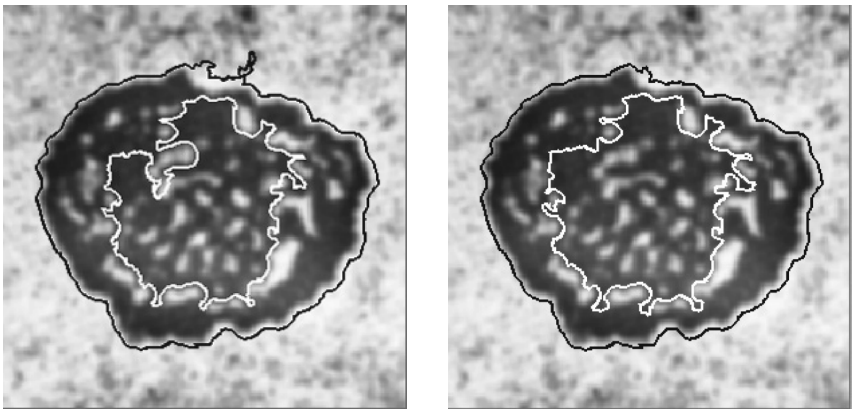

(a) (b)

Figure 15. (a) Outer and inner fronts just before the time point at which they undergo topological changes. (b) Fronts right after the topological changes. Adapted with permission from Giraldi GA, Strauss E, Oliveira AF. 2003. Dual-T-snakes model for medical imaging segmentation. *Pattern Recognit Lett* **24**(7):993–1003. Copyright ©2003, Elsevier.

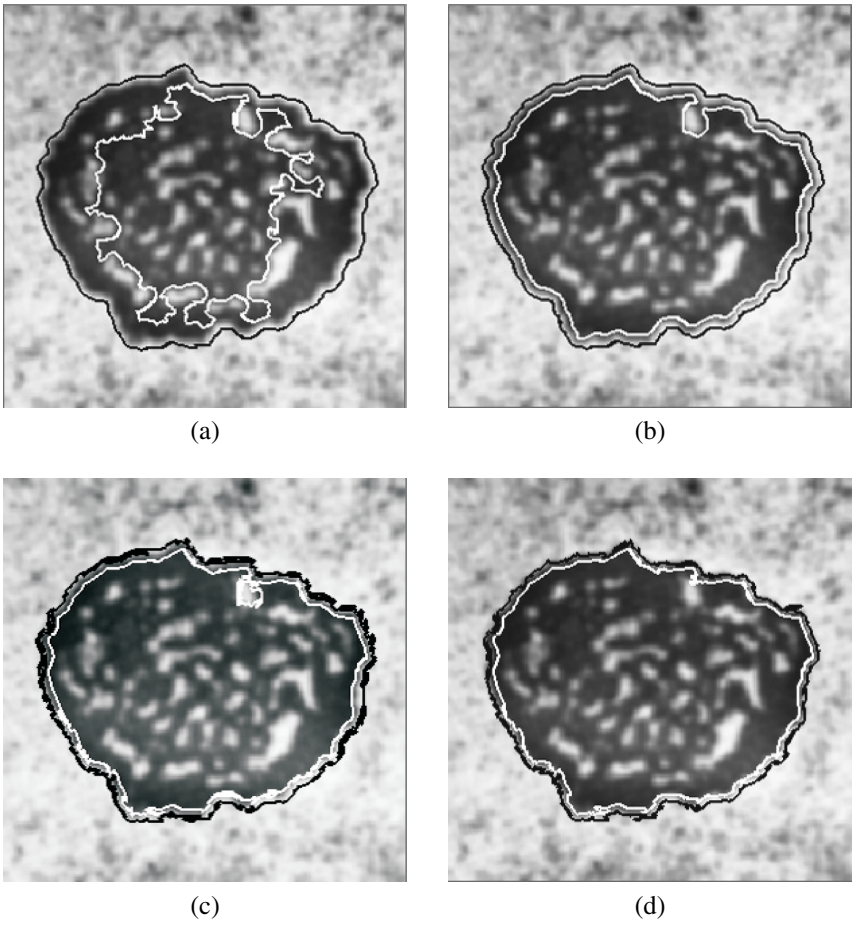

Figure 16. (a) Position of the fronts after 500 interactions. (b) Fronts stop moving due to artifacts. (c) Result after turning on the driving velocity for 20 interactions. (d) Dual-Level-Set result. Adapted with permission from Giraldi GA, Strauss E, Oliveira AF. 2003. Dual-T-snakes model for medical imaging segmentation. *Pattern Recognit Lett* **24**(7):993–1003. Copyright ©2003, Elsevier.

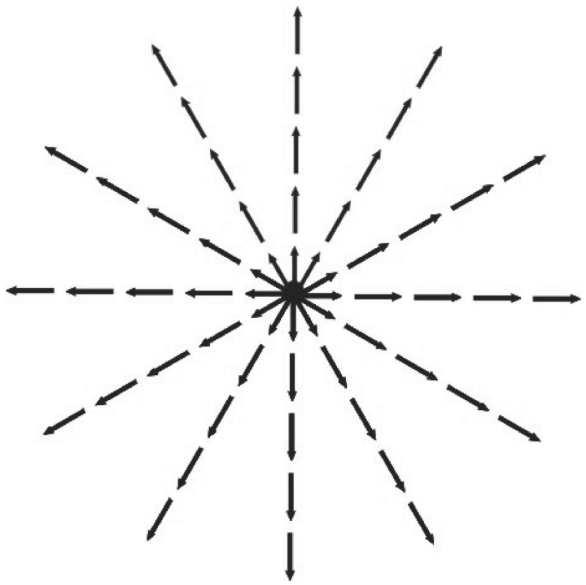

Figure 17. Radial field used to define driving velocity.

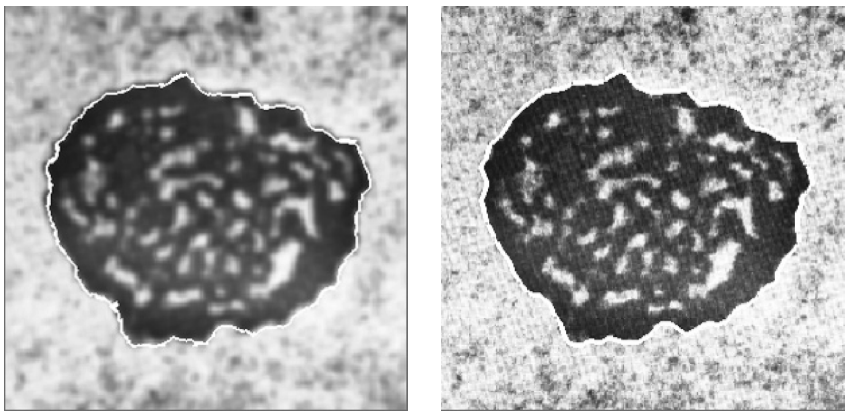

(a) (b)

Figure 18. (a) Original image with a cell nucleolus. (b) Initial fronts. Adapted with permission from Giraldi GA, Strauss E, Oliveira AF. 2003. Dual-T-snakes model for medical imaging segmentation. *Pattern Recognit Lett* **24**(7):993–1003. Copyright ©2003, Elsevier.